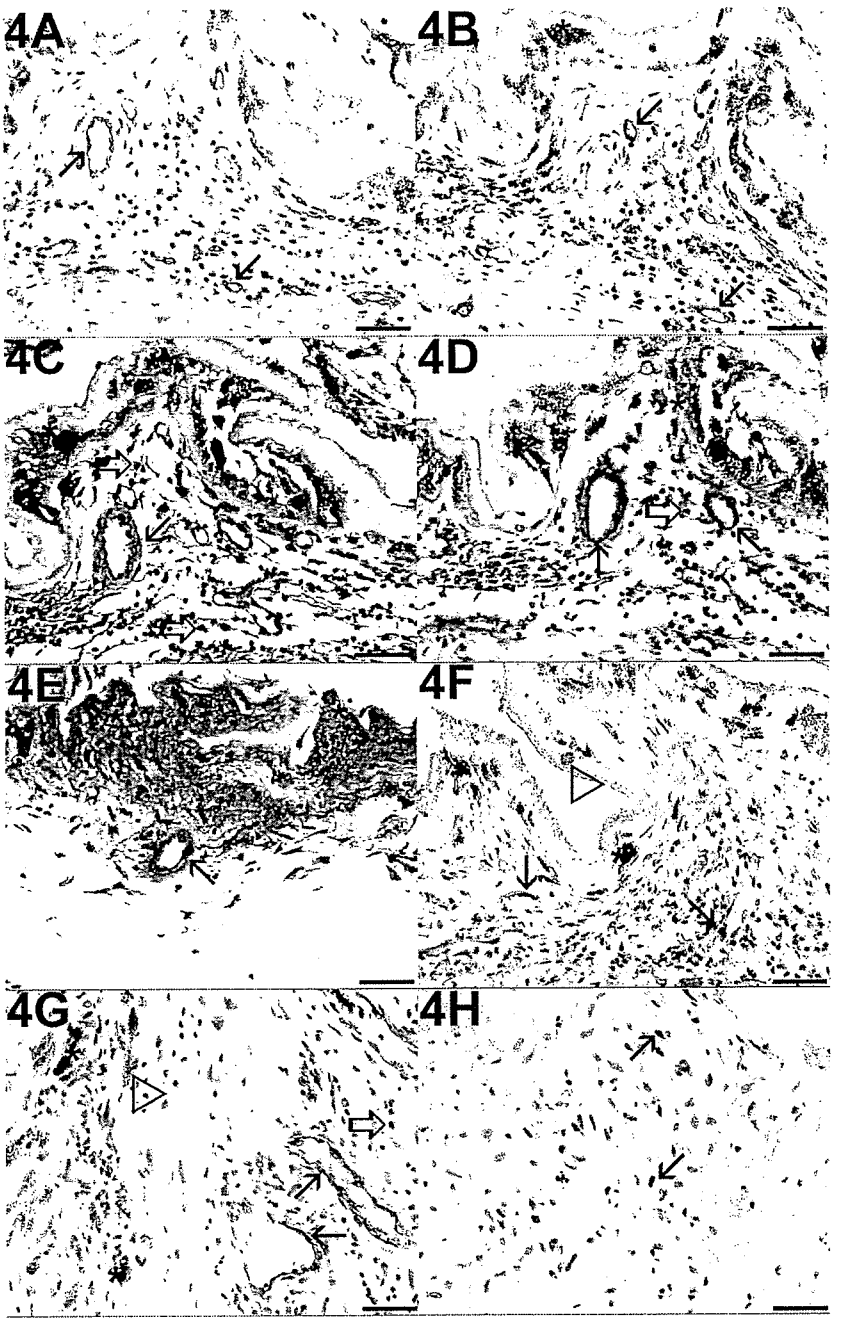
4A
4B
4C
4D
4E
4F
4G
4H

Graefe's Arch Clin Exp Ophthalmol
DOI 10.1007/s00417-005-0177-2

CLINICAL INVESTIGATION

Enrique Adan Sato
Yuichiro Ohtake
Kei Shinoda
Yukihiko Mashima
Itaru Kimura

Decreased blood flow at neuroretinal rim of optic nerve head corresponds with visual field deficit in eyes with normal-tension glaucoma

Received: 6 May 2005
Revised: 14 September 2005
Accepted: 6 October 2005

E. A. Sato · Y. Ohtake · K. Shinoda · Y. Mashima · I. Kimura (✉)
Department of Ophthalmology,
Keio University School of Medicine,
35 Shinanomachi, Shinjuku-ku,
160-8582 Tokyo, Japan
e-mail: kimura@sc.itc.keio.ac.jp
Tel.: +81-3-33531211
Fax: +81-3-33598302

K. Shinoda
Laboratory of Visual Physiology,
National Institute of Sensory Organs,
Tokyo, Japan

Abstract *Purpose:* To determine the relationship between the blood flow parameters of the optic disc rim and the glaucomatous visual field changes. *Design:* Observational cross-sectional study. *Methods:* Tissue blood flow in the neuroretinal rim within the optic disc was determined with the Heidelberg retina flowmeter (HRF) in 54 eyes of 54 patients with normal-tension glaucoma (NTG). Patients were selected whose visual field defects were confined to either the superior or inferior hemifield. Blood flow measurements were made in a 10°×2.5° area of the superior and inferior neuroretinal rim within the optic disc. The mean blood flow (MBF) was calculated by the automatic full-field perfusion image analyzer program, and the ratio of the MBF in the superior to the inferior rim areas (the S/I ratio) was calculated from the same HRF image in order to minimize the variation in measurement conditions. *Results:* Inferior rim blood flow was less than superior rim blood flow in patients with superior hemifield defect, and superior rim blood flow was reduced compared to inferior in patients with inferior hemifield defect. The mean S/I ratios of the MBF in the patients with superior hemifield defect (1.46, n=37) was significantly higher than that in the patients with inferior hemifield defect (0.79, n=17; P<0.0001, Mann–Whitney U-test). *Conclusions:* The blood flow in the neuroretinal rim was found to correspond to the regional visual field defect in eyes with NTG. Reductions in flow were associated with reductions in function.

Keywords Neuroretinal rim · Normal-tension glaucoma · Tissue blood flow · Visual field defect

Introduction

Eyes diagnosed with glaucoma are characterized by progressive optic neuropathy, excavation of the optic nerve head (ONH), and glaucomatous visual field losses. It is known that superior defects will be associated with inferior nerve fiber loss, and inferior defects associated with superior nerve fiber loss in ONH. The exact mechanism causing these changes has not been established, and mechanical theory and vascular theory have been proposed [4, 6, 22, 29, 32]. However, a growing body of evidence has accumulated that supports the idea that the glaucomatous optic nerve head damage results from ocular perfusion deficits [5, 10, 13, 20, 31].

Recently, Logan et al. measured tissue blood flow in a 10 pixel×10 pixel box 200 μm from the disc margin in each quadrant, using the Heidelberg retina flowmeter (HRF, Heidelberg Engineering, Heidelberg, Germany) [23]. They reported that glaucomatous subjects had lower retinal hemodynamic values than control subjects in these areas. The retinal nerve fiber layer in the inferior sector of the retina and the tissue in the inferior sector of the ONH have been reported to have lower blood flow/unit nerve tissue volume than does the superior sector [11]. This would mean that the retinal ganglion cells and their axons in the inferior retina are more vulnerable to circulatory alterations than those in the superior retina. This corresponds with clinical findings that glaucomatous visual field defects are more commonly

found in the superior visual field than in the inferior field [12]. In addition, Yamazaki and Drance, using color Doppler imaging, reported that eyes with NTG and progressive visual field defects have significantly lower blood flow velocities and higher resistive indices in the short posterior ciliary and retinal arteries than eyes with relatively stable visual fields [34].

These studies suggest that alterations in the circulation in glaucomatous eyes are associated with the glaucomatous visual field changes. However, only limited information is available on whether the retinal hemodynamics is altered in eyes with glaucomatous visual field changes [7, 14, 34]. In addition, one weakness of most previous studies on retinal blood flow using the HRF is the sampling technique used to measure the blood flow [15, 16, 23, 25, 28]. A small (10×10) pixel frame was used, and this was most likely not large enough to counteract the physiological variability of blood flow across the retina. In addition, a slight shift of the site of measurement can lead to very different results, as have been reported [3, 17, 23].

We thus evaluated tissue blood flow in patients with NTG and investigated the relationship between the blood flow characteristics around the optic disc with the retinal sensitivity determined by Humphrey visual field testing. To overcome the limitations of the earlier studies we used the automatic full-field perfusion image analyzer (AFFPIA) to minimize the bias due to the heart beat-associated pulsation and the spatial heterogeneity [27].

Patients and methods

Subjects

There were 54 patients with NTG, 25 men and 29 women, whose ages ranged from 35 years to 78 years (60.1±11.7 years; mean ± standard deviation). The procedures used conformed to the tenets of the Declaration of Helsinki, and informed consent was obtained from all patients before the measurements were taken.

All the patients were newly diagnosed as having NTG, and none had received any drug for the glaucoma. Ophthalmological examinations also showed that they had: normal open angle, glaucomatous ONH cupping, and reproducible Humphrey visual field defects with the 30-2 full-threshold strategy program. (Humphrey Instruments., San Leonardo, Calif., USA). Suspicious cases were confirmed as having NTG glaucoma by two specialists (Y.O. and I.K.) from the fundus photographs and visual fields.

The intraocular pressure (IOP) was measured with the Goldmann applanation tonometer. The IOPs were within the normal range (<21 mmHg) at all times including the five baseline measurements and the values obtained during diurnal testing (every 3 h from 6:00 to 24:00 h).

The exclusion criteria were ophthalmic diseases such as uveitis, ocular trauma, diabetic retinopathy and any other ocular pathologic finding detected by slit-lamp and indirect ophthalmoscopic examination. In addition, patients with any history of intraocular or laser surgery, systemic hypertension, cardiovascular diseases, a distance refractive error (spherical equivalent) of more than 6.0 diopters (D) and astigmatism of more than 2.0 D were excluded. Patients receiving any medications such as corticosteroids, β-blockers, calcium channel blockers, angiotensin-converting enzyme inhibitors, platelet active agents, and carbonic anhydrase inhibitors were also excluded.

Humphrey visual field test

Patients with NTG whose visual field defects were confined to either the superior or inferior hemifield were selected. Candidates had to have had a visual field examination by the 30-2 program of the Humphrey perimeter at least twice and had to have scores that were reliable (fixation loss, false-positive or negative -response <33%), and reproducible results with a mean deviation (MD) above −12 dB.

The patients were divided into two groups from the modified criteria stated by Anderson and Patella [1]: those whose defect was confined to the superior hemifield (S-group), and those with a defect in the inferior hemifield (I-group). We defined a "superior hemifield defect" as that in which at least three contiguous non-edge points on the pattern deviation of the Humphrey 30-2 full-threshold superior visual field were abnormal, with a $P<0.05$ for the pattern deviation in the appropriate visual field and no abnormal points detected in the inferior hemifield. If both eyes of a patient satisfied these criteria, the right eye was chosen for analysis.

The demographics of both groups are shown in Table 1. The differences in the gender, age, and IOP between both groups were not statistically significant.

Experiment design

A cross-sectional study design was followed. The Humphrey visual field tests were performed with the 30-2 full threshold strategy to determine whether visual field defects were present. Confocal scanning laser Doppler flowmetry (SLDF)

Table 1 Demographics of S-group and I-group

Characteristic	S-group	I-group
Gender	Male 17; female 20*	Male 8; female 9*
Mean age (range) (years)	62.2±11.3 (38~77)**	55.6±11.7 (35~75)y/o**
Mean IOP (range) (mmHg)	16.6±2.3 (11~20)***	16.7±2.2 (12~20)***mmHg

*P=0.940, **P=0.054, ***P=0.895

was performed to determine the hemodynamic parameters of the neuroretinal rim within the optic disc, using HRF. The interval between the visual field tests and SLDF measurements was less than 3 days for all eyes.

The total pattern deviation values (in decibels) of the visual field, as determined by the Humphrey perimeter, were summed for the superior and the inferior hemifield and were evaluated to determine the relationship between the blood flow and the glaucomatous visual field damages.

Blood flow measurements

After the IOPs had been measured by applanation tonometry, blood flow measurements were made by confocal SLDF using the HRF. The areas measured were the superior and inferior areas at the margin of the ONH, including a measurement of a 10°×2.5° retinal area with 256 points × 64 lines.

The principle, validity, and reliability of SLDF to measure ocular blood flow have been published [24, 26]. The pixelation of the instrument was 10 μm, with a wavelength of 795 nm; the intensity was 100 μW, and the data acquisition time was 2.048 s. Every line was scanned 128 times with a line-sampling rate of 4,000 Hz. The final data set contained 128 discrete recordings at each pixel, and the data were converted into a continuous wave function for each pixel.

The signals were fast-Fourier transformed to obtain the power spectrum of the multiple frequency shift components. Images were included automatically by AFFPIA if the direct current (DC) value within the measurement area was between 40 arbitrary units and 228 arbitrary units. A power spectrum was computed for each pixel by the SLD flowmeter. This spectrum enabled the operator to compute the variables of blood volume, flow, and velocity.

Blood flow measurements were obtained from at least three recordings for each eye at each session by the same experienced investigator. Three good-quality images from each session were selected for statistical analysis. The coefficient of variation (CV) of the three measurements, calculated by SLDF, was used to evaluate intra-session reproducibility. All measurements were made without pupillary dilation. Subjects were asked to use the partner eye to fix on a distant target during the examination. A moveable fixation point was used to allow the positioning of the examined eye. Several mapped images were then acquired in the superior and inferior optic disc rim areas. Great care was taken to measure the corresponding retinal areas repeatedly by taking visible vessels and optic disc margin as landmarks on the video-monitor.

All images were analyzed by the same masked observer. Poor-quality images, mainly due to gross eye movements and poor fixation, were excluded from the analysis.

The mean blood flow (MBF) was calculated by the AFFPIA as an indicator of tissue microcirculation in the neuroretinal rim area by analyzing the MBF in the area between the two concentric semicircular lines along the neuroretinal rim contour. The outer circle of the AFFPIA was adjusted to the neuroretinal contour, and the inner circle was adjusted to the margin of the disc cupping as well as possible in each case (Fig. 1). The patients whose disc shape was far from circular, such as a tilted disc, or whose disc had peripapillary atrophy were excluded. The values are given in arbitrary units (AU). The relative MBFs or ratio of the superior scanned area to the inferior scanned area (S/I ratio) in the same HRF image were evaluated. The investigator analyzing the hemodynamic variables had no knowledge of the patient's clinical findings (i.e., visual field defect).

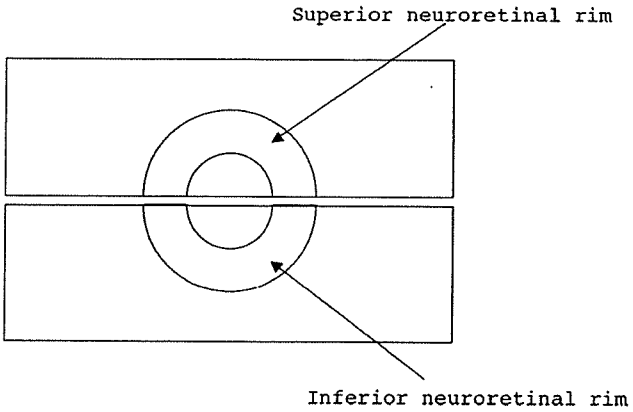

Fig. 1 Measurement regions (10°×2.5°) around the disc divided into superior and inferior areas. The outer circle of the AFFPIA was adjusted to the neuroretinal contour and the inner circle was adjusted to the margin of the disc cupping as well as possible in each case. Each measurement was performed three or more times and analyzed by scanning laser Doppler flowmetry

Evaluation of ocular perfusion pressure

The ocular perfusion pressure (OPP) is defined as the difference between the pressure in the arteries entering the tissue and the veins leaving it. The OPP can be approximated by the following formula using the mean blood pressure (BPm) and the IOP, before and after HRF measurements.

Table 2 Total pattern deviation values of S-group and I-group. The data are presented as decibels

Region	S-group (n=37)	I-group (n=17)
Superior hemifield	−510.6±212.4*	−60.4±36.4**
Inferior hemifield	−75.9±59.9*	−347.8±163.4**
Entire field	−586.5±238.8***	−408.2±171.1***

*P<0.0001, **P=0.0003, ***P=0.0132

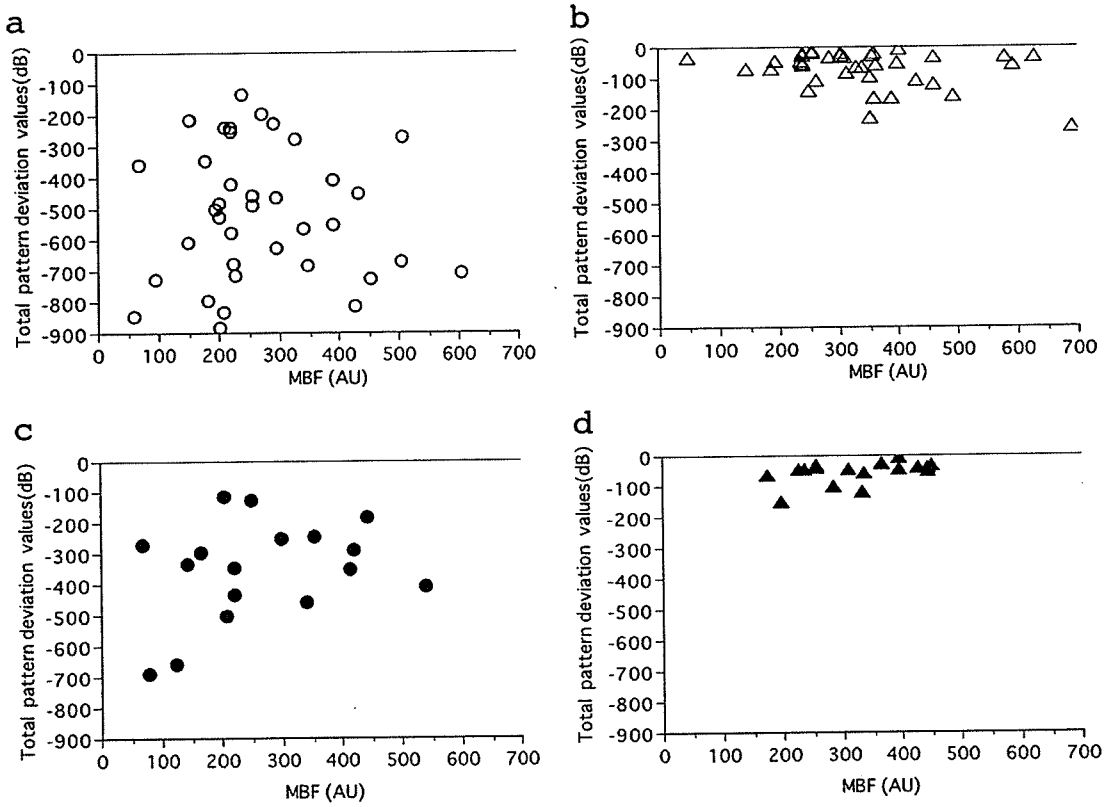

Fig. 2 Correlation between MBF and total pattern deviation value of the corresponding hemifield. **a** Total pattern deviation value of superior hemifield and inferior MBF in S-group. **b** Total pattern deviation value of inferior hemifield and superior MBF in S-group. **c** Total pattern deviation value of inferior hemifield and superior MBF in I-group. **d** Total pattern deviation value of superior hemifield and inferior MBF in I-group. No significant correlation was found between MBF and total pattern deviation value in either area of either group

$$OPP = 2/3 \times BPm - IOP$$
$$BPm = BPd + 1/3 \times (BPs - BPd)$$

where BPd and BPs are the diastolic blood pressure and systolic blood pressure, respectively.

Statistical methods

Three selected SLDF images were analyzed, and the average of the measurements from the three images was used for statistical analysis. The total pattern deviation values in the superior and inferior areas were compared, using the Wilcoxon signed-rank test. The MBF values in the superior and inferior areas were compared, using the Wilcoxon signed-rank test. Spearman's correlation coefficient was calculated to determine the correlation between the total pattern deviation values in Humphrey visual field testing and MBF value in the corresponding neuroretinal rim area. The S/I ratio of the MBF between the S-group and the I-group was compared by the Mann–Whitney U test. A P value of <0.05 was considered statistically significant, and the Bonferroni procedure was used in order to adjust the alpha value.

Results

The total pattern deviation values in the entire, superior hemifield, and inferior hemifield are shown in Table 2. In the S-group, the total pattern deviation value in the superior hemifield was significantly lower than that of the inferior hemifield ($P<0.0001$; Wilcoxon signed-rank test). In the

Table 3 MBF values and S/I ratios of S-group and I-group. Data are presented as arbitrary units

Parameter	S-group(n=37)	I-group(n=17)
Superior neuroretinal rim	342.4±134.4*	263.3±135.4**
Inferior neuroretinal rim	271.2±123.5*	325.6±91.4**
S/I ratio	1.46±0.86***	0.79±0.31***

*P=0.0001, **P=0.0036, ***P<0.0001

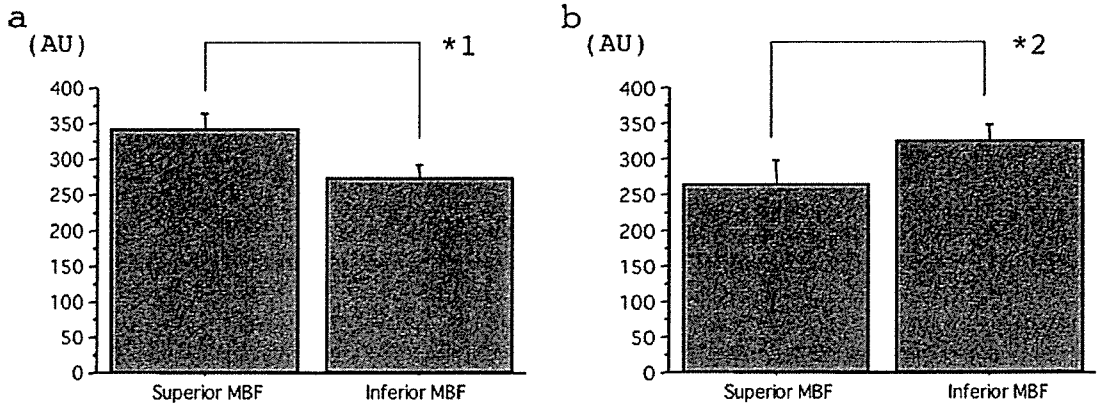

Fig. 3 Averaged MBF of each area in both groups. **a** S-group. The mean of the superior MBF was significantly higher than that of the inferior MBF (**1P*= 0.0001). **b** I-group. The mean of the inferior MBF was significantly higher than the superior MBF (**2P*= 0.0036)

I-group, the total pattern deviation value was reversed, i.e., the total pattern deviation value in the superior hemifield was significantly higher than that of the inferior hemifield (P=0.0003; Wilcoxon signed-rank test).

The MBF in each area was not significantly correlated with the total pattern deviation values of the corresponding field in either group (Fig. 2).

The average MBF in each area is shown in Table 3. The mean coefficient of variation of the three measurements of MBF for the superior and inferior neuroretinal rim was 19.9% and 15.9%, respectively. In the S-group the average MBF in the superior rim area was significantly higher than that in the inferior rim (Fig. 3a, P=0.0001; Wilcoxon signed-rank test), and in the I-group the mean MBF in the inferior rim was significantly higher than that in the superior rim (Fig. 3b; P=0.0036; Wilcoxon signed-rank test).

The mean ratio of the superior to inferior MBF (S/I ratios) in the S-group was significantly higher than that in the I-group (P<0.0001; Mann–Whitney U test; Fig. 4).

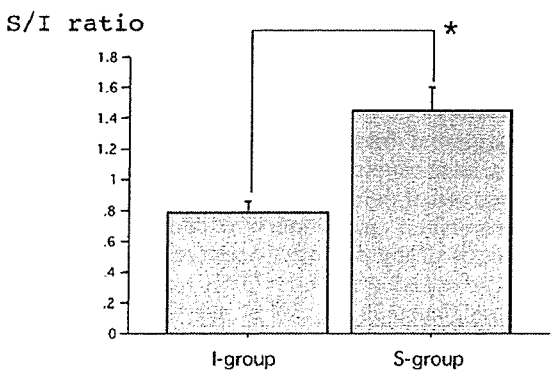

Fig. 4 Mean S/I ratios of MBF in both groups. The S/I ratio in the S-group was significantly higher than that in the I-group (P<0.0001)

There was no significant change in the perfusion pressure in each subject before or after the HRF measurements.

Discussion

The prevalence of patients with NTG in Japan is considerably higher than that of those with primary open angle glaucoma (POAG) and ocular hypertension [18]. Evidence has been accumulating that shows that glaucomatous optic nerve damage is a multi-factorial process [4–6, 10, 13, 30, 32, 33]. It was reported that neuroretinal rim MBF is decreased in NTG patients in comparison with healthy subjects [20]. In our patients a significant reduction in the ONH circulation was found, and the area of reduced blood flow corresponded with the visual field defect. These findings are in good accord with previous studies that show a correlation between glaucomatous visual field loss and alterations of the ONH or retrobulbar circulation in glaucomatous patients [29, 35]. Thus, our findings are consistent with the vascular theory.

Different techniques have been used to determine the vascular condition of the retina and ONH in glaucomatous eyes, but technology has not been available to characterize the perfusion of the ONH in detail [5, 9]. Although the blood supply on the rim area is rather complex, it is reasonable that the blood flow on the superior area of the ONH in normal eyes is as much as that of the inferior area, as has been reported by Harris et al. [11].

The main source of blood supply to the ONH comes from the posterior ciliary arteries, except for the surface nerve fiber layer, which is supplied by the retinal circulation [14]. The blood flow values in the disc rim areas obtained by SLDF are, therefore, a mixture of retinal and choroidal blood because the depth of laser penetration is approximately 400 μm. However, it is possible that the glaucomatous thinning of the neuroretinal rim will allow a deeper

scanning depth, and contributions from the prelaminar region become higher. Our findings that the blood flow values were correlated with the visual field changes indicate that we were indirectly assessing the physiological status of the retinal nerve fiber layer and neighboring retinal ganglion cells.

Many previous studies that investigated retinal blood flow with the HRF used the default 10 pixel×10 pixel sampling box [15, 23, 25, 28]. This method gave results with a high coefficient of variation when tests were repeated weekly. Therefore, this size is generally considered not to be suitable. The blood flow within the measuring window depends strongly on its position and varies with location and time. A recently developed computer program, called AFFPIA, can be used to perform a full-field analysis of the image obtained with the HRF [24]. This program incorporates a method of deleting recordings containing saccades from the analysis, which then reduces the rate of image rejection.

Eyes with focal defects often have notches, and it is difficult to exclude the areas of notches from the blood flow measurement areas. However, the ratio of notch area to rim area is generally very small. We think the influence of notches may be minimal.

One of the limitations of our study using AFFPIA is that measurements could not be made on the nasal or temporal neuroretinal rim area. However, the correlation between the visual field defect and the reduced blood flow supports the idea that abnormalities of the microcirculation of the ONH, retina, and choroid play a considerable role in the etiology of NTG. Our observations mean that reductions in flow were associated with reductions in function. These are in good accord with those of Arend et al., who found altitudinal visual field asymmetry coupled with altered retinal circulation using digital image analysis of fluorescein angiograms in patients with NTG [2].

The number of eyes that were classified into the S-group was higher than that of the I-group. In addition, the total pattern deviation values for the entire field was significantly lower in the S-group than in the I-group. These findings correspond with the earlier occurrence of visual field loss in the arcuate area, especially in the superior hemifield and the preferential damage to the inferior–temporal quadrant [8, 12, 19, 31].

There are a number of factors that can affect the SLDF measurements, e.g., structural changes that occur in glaucomatous eyes, and opacities of the crystalline lens or vitreous that can affect the intensity and coherence of the laser light reaching the scanned area [21]. Also, antiglaucoma medications can affect the ocular circulation [21]. To eliminate these factors we selected newly diagnosed early NTG patients who had not received any antiglaucoma medication. In addition, eyes with mild or moderate cataracts, and pseudophakic eyes, were excluded. The S/I ratio was used instead of absolute values to avoid the effect of interocular variability. Even in glaucomatous patients with asymmetrical interocular microcirculation, the S/I ratio can be a useful method to assess regional ocular circulation impairments if the eye has glaucomatous changes in the superior or inferior hemifield.

The increased IOP is known to be a major risk factor for optic nerve damage. However, we investigated NTG patients to minimize the known effect of IOP on ocular microcirculation.

The juxtapapillary retinal blood flow was reported to be reduced in association with the structural damage of the ONH in patients with POAG and NTG by SLDF [23]. Michelson et al. observed that a significant inverse relationship existed between the cup-to-disk ratio (C/D) and ONH blood flow but no relationship between the C/D and juxtapapillary retinal blood flow in POAG patients [25]. In contrast, Yamazaki and Drance reported a significant decrease in the blood flow velocities and increase of resistive indices in the retrobulbar arteries in eyes with progressive visual field defect in patients with NTG but not in glaucomatous patients with increased IOP [34]. Yaoeda et al. reported a significant correlation between a decrease in ONH blood flow velocity, as measured by laser speckle flowgraphy, and visual field loss in the NTG group but not in the POAG group [35]. They concluded that the circulatory parameters of the retrobulbar arteries or of the ONH may be associated with the visual field defects in NTG but may be less involved in the deterioration of the glaucomatous patients with initially increased IOP [34, 35]. These differences might be due to other factors influencing the ocular perfusion. Further investigations designed to recognize the entire range of possible circulatory factors, including IOP and medication, will be helpful to determine the contribution of the change in perfusion to the pathogenesis or progression of the glaucomatous visual field in POAG.

It is not possible to state whether the changes in the blood flow in our patients were an early manifestation of the disease process or if the extensive loss of axons in the ONH resulted in the altered blood flow. Logan et al. reported that the retinal circulation in glaucoma patients, identified by HRT parameters as having a normal neuroretinal rim, is reduced [23]. Piltz-Seymour et al. have reported that open angle glaucoma suspects without manifest visual field defects have decreased blood flow similar to that seen in glaucoma patients with visual field defects [29]. Furthermore, Zink et al. have shown that lower ONH volume in the inferior temporal rim is associated with a faster progression in the corrected pattern standard deviation (CPSD) values of Humphrey visual field testing [36]. These findings suggest that the impaired circulation is a causative factor in the pathogenesis of the disease. Therefore, retinal blood flow assessment in and around the ONH may be important for identifying glaucoma patients at risk for future glaucomatous visual field progression, determining disease severity, or monitoring treatment interventions.

References

1. Anderson DR., Patella VM (1999) Interpretation of a single field. In: Anderson DR., Patella VM (eds) Automated static perimetry, 2nd edn. Mosby, St Louis, pp 121–190
2. Arend O, Remky A, Cantor LB, Harris A (2000) Altitudinal visual field asymmetry is coupled with altered retinal circulation in patients with normal pressure glaucoma. Br J Ophthalmol 84:1008–1012
3. Chung HS, Harris A, Kagemann L, Martin B (1999) Peripapillary retinal blood flow in normal tension glaucoma. Br J Ophthalmol 83:466–469
4. Drans SM, Anderson DR (1995) Optic nerve blood flow. In: Drans SM, Anderson DR (eds) Optic nerve in glaucoma. Kugler, Amsterdam, New York, pp 311–331
5. Flammer J, Orgul S (1998) Optic nerve blood-flow abnormalities in glaucoma. Prog Retin Eye Res 17:267–289
6. Gramer E, Tausch M (1995) The risk profile of the glaucomatous patient. Curr Opin Ophthalmol 6:78–88
7. Grunwald JE, Piltz J, Hariprasad SM, DuPont J (1998) Optic nerve and choroidal circulation in glaucoma. Invest Ophthalmol Vis Sci 39:2329–2336
8. Harrington DO (1965) The Bjerrum scotoma. Am J Ophthalmol 59:646–656
9. Harris A, Kagemann L, Cioffi GA (1998) Assessment of human ocular hemodynamics. Surv Ophthalmol 42:509–533
10. Harris A, Chung HS, Ciulla TA, Kagemann L (1999) Progress in measurement of ocular blood flow and relevance to our understanding of glaucoma and age-related macular degeneration. Prog Retin Eye Res 18: 669–687
11. Harris A, Ishii Y, Chung HS, Jonescu-Cuypers CP, McCranor LJ, Kagemann L, Garzozi HJ (2003) Blood flow per unit retinal nerve fibre tissue volume is lower in the human inferior retina. Br J Ophthalmol 87:184–188
12. Hart WM Jr, Becker B (1982) The onset and evolution of glaucomatous visual field defects. Ophthalmology 89:268–279
13. Hayreh SS (1995) The optic nerve head circulation in health and disease. Exp Eye Res 61:259–272
14. Hayreh SS (2001) The blood supply of the optic nerve head and the evaluation of it—myth and reality. Prog Retin Eye Res 20:563–593
15. Hollo G, van den Berg TJ, Greve EL (1996–1997) Scanning laser Doppler flowmetry in glaucoma. Int Ophthalmol 20:63–70
16. Hollo G, Greve EL, van den Berg TJ, Vargha P (1996–1997) Evaluation of the peripapillary circulation in healthy and glaucoma eyes with scanning laser Doppler flowmetry. Int Ophthalmol 20:71–77
17. Hosking SL, Embleton SJ, Cunliffe IA (2001) Application of a local search strategy improves the detection of blood flow deficits in the neuroretinal rim of glaucoma patients using scanning laser Doppler flowmetry. Br J Ophthalmol 85:1298–1302
18. Iwase A, Suzuki Y, Araie M, Yamamoto T, Abe H, Shirato S, Kuwayama Y, Mishima HK, Shimizu H, Tomita G, Inoue Y, Kitazawa Y, Tajimi Study Group, Japan Glaucoma Society (2004) The prevalence of primary open-angle glaucoma in Japanese: the Tajimi Study. Ophthalmology 111:1641–1648
19. Jonas JB, Fernandez MC, Sturmer J (1993) Pattern of glaucomatous neuroretinal rim loss. Ophthalmology 100:63–68
20. Jonas JB, Harazny J, Budde WM, Mardin CY, Papastathopoulos KI, Michelson G (2003) Optic disc morphometry correlated with confocal laser scanning Doppler flowmetry measurements in normal-pressure glaucoma. J Glaucoma 12:260–265
21. Kagemann L, Harris A, Chung HS, Evans D, Buck S, Martin B (1998) Heidelberg retinal flowmetry: factors affecting blood flow measurement. Br J Ophthalmol 82:131–136
22. Kimura I, Shinoda K, Ohtake Y, Tanino T, Mashima Y (2005) Effect of topical isopropyl unoprostone on optic nerve head circulation in normal subjects and in NTG patients. Jpn J Ophthalmol 49:287–293
23. Logan JF, Rankin SJ, Jackson AJ (2004) Retinal blood flow measurements and neuroretinal rim damage in glaucoma. Br J Ophthalmol 88:1049–1054
24. Michelson G, Schmauss B (1995) Two dimensional mapping of the perfusion of the retina and optic nerve head. Br J Ophthalmol 79:1126–1132
25. Michelson G, Langhans MJ, Groh MJ (1996) Perfusion of the juxtapapillary retina and the neuroretinal rim area in primary open angle glaucoma. J Glaucoma 5:91–98
26. Michelson G, Schmauss B, Langhans MJ, Harazny J, Groh MJ (1996) Principle, validity, and reliability of scanning laser Doppler flowmetry. J Glaucoma 5:99–105
27. Michelson G, Welzenbach J, Pal I, Harazny J (1998) Automatic full field analysis of perfusion images gained by scanning laser Doppler flowmetry. Br J Ophthalmol 82:1294–1300
28. Nicolela MT, Hnik P, Drance SM (1996) Scanning laser Doppler flowmeter study of retinal and optic disk blood flow in glaucomatous patients. Am J Ophthalmol 122:775–783, erratum in Am J Ophthalmol 123:575
29. Piltz-Seymour JR, Grunwald JE, Hariprasad SM, Dupont J (2001) Optic nerve blood flow is diminished in eyes of primary open-angle glaucoma suspects. Am J Ophthalmol 132:63–69
30. Quigley HA, Addicks EM (1981) Regional differences in the structure of the lamina cribrosa and their relation to glaucomatous optic nerve damage. Arch Ophthalmol 99:137–143
31. Shields MB (1998) Visual function in glaucoma. In: Shields MB (ed) Shields' textbook in glaucoma, 3rd edn. Williams and Wilkins, Baltimore, pp 180–186
32. Spaeth GL (1971) Pathogenesis of visual loss in patients with glaucoma. Pathologic and sociologic considerations. Trans Am Acad Ophthalmol Otolaryngol 75:296–317
33. Stamper RL, Lieberman MF, Drake MV (1999) Optic nerve anatomy and pathophysiology. In: Stamper RL, Lieberman MF, Drake MV (eds) Becker-Shaffer's diagnosis and therapy of the glaucomas. Mosby, St Louis, pp 177–190
34. Yamazaki Y, Drance SM (1997) The relationship between progression of visual field defects and retrobulbar circulation in patients with glaucoma. Am J Ophthalmol 124:287–295
35. Yaoeda K, Shirakashi M, Fukushima A, Funaki S, Funaki H, Abe H, Tanabe N (2003) Relationship between optic nerve head microcirculation and visual field loss in glaucoma. Acta Ophthalmol Scand 81:253–259
36. Zink JM, Grunwald JE, Piltz-Seymour J, Staii A, Dupont J (2003) Association between lower optic nerve laser Doppler blood volume measurements and glaucomatous visual field progression. Br J Ophthalmol 87:1487–1491

Graefe's Arch Clin Exp Ophthalmol
(2007) 245: 305–308

CASE REPORT

DOI 10.1007/s00417-005-0236-8

Takefumi Yamaguchi
Makoto Inoue
Susumu Ishida
Kei Shinoda

Detecting vitreomacular adhesions in eyes with asteroid hyalosis with triamcinolone acetonide

Received: 12 September 2005
Revised: 23 October 2005
Accepted: 4 December 2005
Published online: 13 January 2006

T. Yamaguchi · M. Inoue (✉) ·
S. Ishida · K. Shinoda
Department of Ophthalmology,
Keio University, School of Medicine,
35 Shinanomachi, Shinjuku-ku,
Tokyo, 160-8582, Japan
e-mail: inoshin@sc.itc.keio.ac.jp
Tel.: +81-33353-1211
Fax: +81-33359-8302

Abstract *Background:* To report the incidence of posterior vitreous detachments (PVDs) and the surgical results of vitrectomy with intravitreal triamcinolone acetonide (TA) to detect vitreomacular adhesions in eyes with asteroid hyalosis (AH).
Methods: Ten eyes of nine patients with AH underwent vitrectomy, six eyes with TA and four without TA. The presence of a PVD was determined preoperatively by ultrasound echography (USE) and intraoperatively by microscopic observations. The postoperative best-corrected visual acuities (BCVA) were evaluated.
Results: The BCVA was improved by >2 Snellen lines in nine eyes and maintained at 20/20 with symptomatic improvements in the other eye. A vitreomacular adhesion was clearly seen during TA-assisted vitrectomy, and none was seen when TA was not used, even though preoperative USE showed an incomplete PVD in all eyes. The BCVA was not significantly better in eyes with TA-assisted vitrectomy than without TA-assisted vitrectomy. In one eye with vitrectomy without TA, a second surgery was required for a persistent cystoid macular edema and an epiretinal membrane. The BCVA and the edema in this eye improved after removing the epiretinal membrane. *Conclusions:* All (ten) of the eyes with AH were found to have a vitreomacular adhesion by preoperative USE and intraoperative microscopic observations. The residual vitreous over the macula is more easily detected and removed after intravitreally injected TA, but the visual acuities were not significantly different from eyes without TA.

Keywords Asteroid hyalosis · Triamcinolone acetonide · Vitreous · Vitrectomy · Vitreomacular traction

Introduction

Asteroid hyalosis (AH) is a relatively common vitreous disease in elderly patients and is characterized by deposits of glistening, lipid-containing calcium bodies in the vitreous [4]. A precise assessment of the retina may be difficult because the asteroid bodies can hamper a clear view of the posterior segment. AH does not cause significant visual impairment in most cases, but vitrectomy is beneficial when other ocular pathologic conditions are present [2, 5].

An intravitreal application of triamcinolone acetonide (TA) during vitrectomy, termed TA-assisted vitrectomy, makes the transparent vitreous gel more visible, which is helpful in the complete removal of the vitreous [6]. The purpose of this study was to determine the incidence of posterior vitreous detachments (PVDs), and the efficacy of TA-assisted vitrectomy to detect vitreomacular adhesions in eyes with AH.

Materials and methods

Ten eyes of nine patients (seven men and two women) with AH that led to visual disturbances or metamorphopsia underwent vitreous surgery by one of the authors (M.I.). Their

ages ranged from 48 to 79 years (mean 65.0±11.3 years), and the follow-up period ranged from 6 to 48 months (26.1± 12.7 months). Five eyes with mild lens opacities preoperatively had the lens extracted during the vitreous surgery to avoid a second surgery because of visual deterioration through progression of the nuclear cataract. Three eyes were pseudophakic, and the other two eyes were phakic with minimal lens opacity preoperatively.

All patients were fully informed about the purpose and possible complications of the treatment, and signed an informed consent. The Ethics Committee of Keio University approved the use of TA based on recommendation of the Institutional Review Board. The procedures used conformed to the tenets of the Declaration of Helsinki.

TA-assisted vitrectomy was performed to determine if residual vitreous cortex was present at the macula in six eyes. These were consecutive eyes and not randomly selected. Approximately 0.25 ml (10 mg) of TA (Kenacort-A, 40 mg/ml; Bristol Myers KK, Tokyo, Japan) was aspirated into a 1 ml syringe. The syringe was placed on a counter for several minutes, and the supernatant was removed after the crystals of TA had settled on the bottom to reduce the volume to 0.1 ml. Then BSS was added to make the volume up to 1 ml in the syringe, shaken to mix the TA crystals just before the intravitreal injection. Approximate 0.1 ml of this solution of TA was injected after core vitrectomy, and the TA crystals were aspirated immediately.

The TA crystals made the residual vitreous visible, which greatly aided in its complete removal. In the other four eyes, conventional vitrectomy was performed, and the residual vitreous cortex was carefully aspirated around the area of the macula.

The presence of a PVD was determined by preoperative ultrasound echography (USE, UD-1000; TOMEI Co, Nagoya, Japan) with or without eye movements, and also confirmed intraoperatively under the surgical microscope.

The postoperative best-corrected visual acuity (BCVA) of the six eyes with TA-assisted vitrectomy was compared with that of the four eyes with vitrectomy without TA. Statistical analysis was performed by unpaired *t*-tests.

Results

High echographic signals from the vitreous indicated the presence of the asteroid bodies, but the high signals were reduced in the premacular space (Fig. 1). This low-signal space was interpreted as being due to a PVD when USE was done without eye movement (static USE). However, a vitreoretinal adhesion with an incomplete PVD was detected in all eyes by observing less movement of the vitreous gel at the macula during USE with eye movements (dynamic USE, Table 1). In one eye, the posterior vitreous was also attached at the optic disc.

Preoperative fluorescein angiography showed macular edema in two eyes (cases 2 and 9). Intraoperative microscopic observations showed an elevation of the fovea in three eyes indicating macular edema, and parafoveal cysts in two eyes indicating cystoid macular edema (CME). The macular edema resolved postoperatively in all eyes.

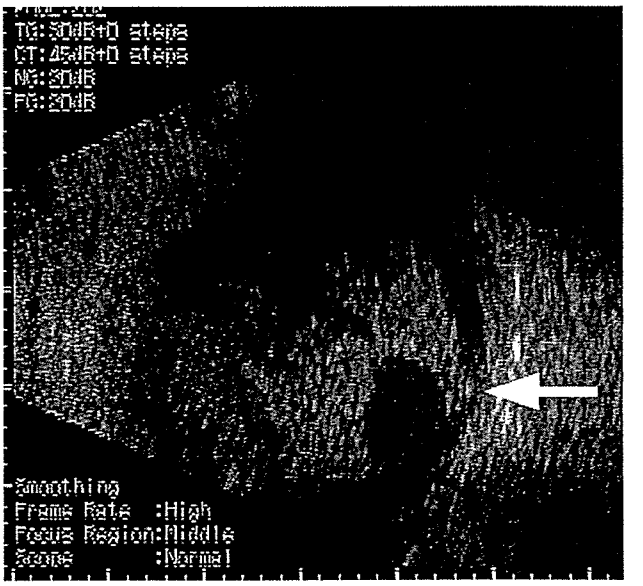

Fig. 1 Ultrasound echogram of case 1. Echogram showing high signals from the vitreous body indicating intravitreal asteroid bodies. Interestingly, the signals are reduced in the area of the vitreomacular attachment (*arrow*) showing low-echo space, suggesting an incomplete posterior vitreous detachment

Preoperatively, a focal adhesion of residual vitreous was observed at the macula in five eyes, and a diffuse vitreous adhesion in one eye, in the six eyes with TA-assisted vitrectomy. An improvement of two or more Snellen lines in the BCVA was achieved in nine eyes, and the mean improvement was 3.5 lines. In the remaining eye, there was an improvement of metamorphopsia while maintaining 20/20 vision. The mean visual improvement was 3.8 lines in eyes with TA-assisted vitrectomy, and 3.0 lines without TA-assisted vitrectomy. This difference in improvement was not significant (P=0.61, unpaired t-test).

The transparent vitreous at the macula was made more visible by the white TA crystals in the six eyes with TA-assisted vitrectomy (Fig. 2). The area of transparent vitreous remaining at the macula corresponded with the low-signal space in the preoperative USE.

As postoperative complications, one eye (case 2) required a cataract extraction for a cataract that developed postoperatively resulting in a visual deterioration to 20/50 from 20/30. The BCVA improved to 20/25 without any recurrent macular edema. Another eye (case 9) had an initial vitrectomy without TA because of macular edema associated with AH. Vision improved to 20/25 from 20/50, but this eye required a second vitrectomy for recurrent persistent CME and an epiretinal membrane resulting in a visual acuity of 20/30. The vision improved to 20/20 after

Table 1 Profile of patients with asteroid hyalosis

Case	Age (years)	Gender	Symptom	VM adhesion	Visual acuity		Surgery	TA-assisted vitrectomy	Pre-op and intra-op condition	Follow-up (months)	Post-op condition
					Pre-op	Post-op					
1 OD	69	W	VA, Met	+	20/100	20/25	PPV, PEA, IOL	+(spot)	Macular edema	30	
1 OS			VA, Met	+	20/60	20/25	PPV, PEA, IOL	+(spot)	Macular edema	30	
2	48	M	VA, Met	+	20/60	20/25	PPV	+(spot)	Macular edema	48	*Cataract
3	79	M	VA	+	20/20	20/20	PPV	+(spot)	Glaucoma	16	
4	63	M	VA	+	20/25	20/18	PPV	+(spot)		6	
5	79	M	VA	+	20/50	20/25	PPV, PEA, IOL	+(diffuse)		8	
6	70	F	VA	+	20/40	20/20	PPV, PEA, IOL	-	CME	32	
7	70	M	VA	+	20/25	20/18	PPV, PEA, IOL	-		30	
8	54	M	VA	+	20/25	20/20	PPV	-		27	
9	53	M	VA, Met	+	20/50	20/20	PPV	-	CME	34	*Cataract, *ERM

M male, *F* female, *VA* symptomatically decreased visual acuity, *Met* symptomatic metamorphopasia, *VM adhesion* vitreomacular adhesion by echogram. *pre-op* preoperative, *post-op* postoperative, *PPV* pars plana vitrectomy, *PEA* phacoemulsification and aspiration, *IOL* insertion of intraocular lens, *TA* triamcinolone acetonide, *+(spot)* residual vitreous visualized as white spot above the macula or diffuse sheet; +(diffuse), *CME* cystoid macular edema, **cataract* cataract developed postoperatively and surgery was performed, **ERM* postoperatively developed epiretinal membrane was removed at the second surgery

the epiretinal membrane was removed and the cataract was extracted during the second vitrectomy. None of the eyes with TA-assisted vitrectomy developed an epiretinal membrane or macular edema postoperatively.

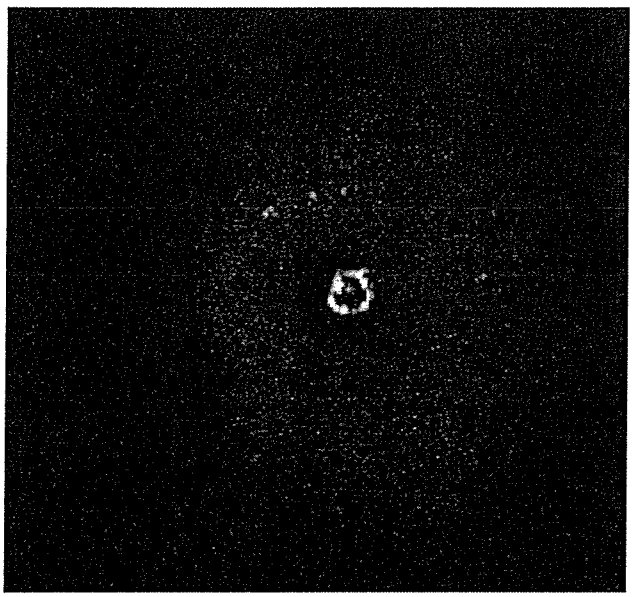

Fig. 2 Intraoperatively microscopic photograph of case 1. Photograph from intraoperative video recording showing vitreomacular adhesion of residual vitreous cortex which was made visible by intravitreally injected triamcinolone acetonide

Discussion

How AH leads to visual symptoms is not completely known. In addition, the indications for vitrectomy in patients with AH have not been definitively determined. Previous studies suggested that vitrectomy was beneficial only in selected patients who required laser photocoagulation, or those who had an unexplained visual loss and a good view of the fundus could not be made. [2] Parnes et al. reported that nine of ten eyes with AH had an improvement of vision of at least one line after vitrectomy, but they did not use TA if macular disease did not exist. [5] These results suggest that vitrectomy alone can improve the visual acuity by simply removing the vitreal opacities.

A PVD is relatively rare in patients with AH and diabetic retinopathy, [8] and a strong adhesion between the retina and vitreous is reported to be present in patients who had undergone vitrectomy for diseases associated with AH and proliferative diabetic retinopathy. [3] This was confirmed in our study, as all of our cases demonstrated a vitreous adhesion at the macula intraoperatively. These findings indicate that AH might increase the degree of vitreomacular adhesion. Interestingly, we did not extract any publications that reported a high incidence of vitreomacular adhesion

detected by ophthalmoscopy or USE in eyes with AH, but without diabetic retinopathy.

Although the number of patients studied was small, residual vitreous cortex was detected by TA-assisted vitrectomy in all of the six eyes with AH, which is higher than that in other retinal diseases undergoing TA-assisted vitrectomy, e.g. 90% in proliferative diabetic retinopathy, 77% in diabetic macular edema, 41% in branch vein retinal occlusion, and 60% in rhegmatogenous retinal detachment [7].

Browning et al. [1] reported a vitreomacular adhesion detected by an optical coherence tomography (OCT) in a patient with diabetic macular edema and AH as was also reported earlier. [3] However, there were no diabetic patients in our series, and a clear OCT image was not obtained from the six eyes with AH that had preoperative OCT. The absence of the high echographic signals from the asteroid bodies in the area of the vitreomacular attachment made it difficult to detect vitreomacular adhesion in static echograms. This absence of signals might be a limitation of USE, but the ophthalmoscopic observations suggested that the vitreous attached to the macula had fewer asteroid bodies than the central vitreous. Thus, conventional vitrectomy may fail to remove vitreomacular adhesions completely because the residual vitreous is less visible with fewer asteroid bodies.

A high incidence of vitreomacular adhesions was found in eyes with AH by preoperative USE and intraoperative observations. Residual vitreous cortex can lead to the formation of epiretinal membranes that cause persistent tangential macular traction, and a complete removal of vitreomacular traction by TA-assisted vitrectomy may provide better visual outcome in vitrectomy in eyes with AH. However, residual vitreous over the macula is better seen and removed with TA, but the visual acuity did not seem to be better with the TA in this small series. In addition, simultaneous cataract surgery for minimal lens opacities may have affected the visual outcomes in the half of the cases. Further studies with functional and morphologic analysis are needed.

Acknowledgement None of the authors has a financial or proprietary interest in any material or methods mentioned.

References

1. Browning DJ, Fraser CM (2004) Optical coherence tomography to detect macular edema in the presence of asteroid hyalosis. Am J Ophthalmol 137:959–961
2. Feist RM, Morris RE, Witherspoon CD et al (1990) Virectomy in asteroid hyalosis. Retina 10:173–177
3. Ikeda T, Sawa H, Koizumi K et al (1998) Vitrectomy for proliferative diabetic retinopathy with asteroid hyalosis. Retina 18:410–414
4. Moss SE, Klein R, Klein BEK (2001) Asteroid hyalosis in a population: the beaver dam eye study. Am J Ophthalmol 132:70–75
5. Parnes RE, Zakov ZN, Novak MA, Rice TA (1998) Virectomy in patients with decreased visual acuity secondary to asteroid hyalosis. Am J Ophthalmol 125:703–704
6. Peyman GA, Cheema R, Conway MD, Fang T (2000) Triamcinolone acetonide as an aid to visualization of the vitreous and the posterior hyaloid during pars plana vitrectomy. Retina 20:554–555
7. Sonoda K, Sakamoto T, Enaida H et al (2004) Residual vitreous cortex after surgical posterior vitreous separation visualized by intravitreous triamcinolone acetonide. Ophthalmology 111:226–230
8. Wasano T, Hirokawa H, Tagawa H et al (1987) Asteroid hyalosis: posterior vitreous detachment and diabetic retinopathy. Ann Ophthalmol 19:255–258

Discordance Between Subjective Perimetric Visual Fields and Objective Multifocal Visual Evoked Potential-Determined Visual Fields in Patients With Hemianopsia

KEN WATANABE, MD, KEI SHINODA, MD, ITARU KIMURA, MD, YUKIHIKO MASHIMA, MD, YOSHIHISA OGUCHI, MD, AND HISAO OHDE, MD

• PURPOSE: To investigate the concordance between subjectively and objectively acquired visual fields in patients with subjectively determined hemianopsia.
• DESIGN: Retrospective observational study.
• METHODS: Ten patients, six men and four women, ranging in age from 28 to 68 years, were studied. Goldmann or Humphrey perimeters were used to obtain the subjectively determined visual fields for up to 25 degrees of eccentricity, and the VERIS Scientific System (Electro-Diagnostic Imaging, San Francisco, California, USA) was used to record multifocal visual evoked potential [VEPs] (mfVEPs) to obtain the objective visual fields. Each of the 60 black-and-white segments of the checkerboard stimulus was alternated according to a binary m sequence. The first slices of the second-order kernels were extracted and analyzed.
• RESULTS: In five cases, the visual field loci where the mfVEPs were within normal limits corresponded to the scotomatous areas obtained by conventional perimetry. In these discordant cases, the lesions (e.g., arteriovenous malformation) were located in the occipital lobe. Two of these cases had a complete recovery of the subjective visual field. The lesions of the concordant cases were located outside the occipital lobe (e.g., pituitary adenoma). In these cases, no visual field improvement was seen. The temporal crescent syndrome was ruled out in patients with posterior lesions by computed tomography (CT) or magnetic resonance imaging (MRI) findings.
• CONCLUSIONS: In some patients with occipital lesions, the subjective and objective visual field results are discordant, and some of them will show a recovery of the visual field deficits. (Am J Ophthalmol 2007;143: 295–304. © 2007 by Elsevier Inc. All rights reserved.)

AJO.com Supplemental Material available at AJO.com.

Accepted for publication Oct 16, 2006.

From the Department of Ophthalmology, Keio University School of Medicine (K.W., K.S., I.K., Y.M., Y.O., H.O.); Laboratory of Visual Physiology, National Institute of Sensory Organs, Tokyo Medical Center (K.S.); and Kamoshita Eye Clinic (H.O.), Tokyo, Japan.

Inquiries to Hisao Ohde, MD, Department of Ophthalmology, Keio University School of Medicine, 35 Shinanomachi, Shinjuku-ku, Tokyo 160-8582, Japan; e-mail: shinodakei@kankakuki.go.jp

VISUAL FIELDS OBTAINED BY THE GOLDMANN AND Humphrey perimeters have been the gold standards for the evaluation of optic nerve diseases and pathologic changes in the visual pathways. These tests are used routinely, but, unfortunately, they are subjective tests. Several methods have been used to try to determine the visual fields objectively; for example, conventional flash and pattern visual-evoked potentials (VEPs),[1–5] vector VEPs,[6] pupillography,[7] scalp topography of VEPs,[8] positron emission tompgraphy,[9] multifocal VEPs (mfVEPs),[10–19] and functional magnetic resonance imaging (MRI).[20–22] However, none of these techniques is used routinely on patients.

The topographic map of the amplitudes of the mfVEPs has been reported to show good agreement or concordance with the results of conventional visual field tests if occipital bipolar electrodes are used.[15,16] Thus mfVEPs have been used on patients with glaucoma to evaluate the functional glaucomatous loss objectively.[19,23,24] In addition, the mfVEPs, summed within the four quadrants, have been used as an objective evaluator of the visual fields in patients with visual field loss.[16,17,19,23,24] However, we have found that the alterations of the topographic map of the mfVEPs are not always in good concordance with the subjectively determined visual fields in some cases with hemianopic field defects.

The purpose of this study was to determine whether the subjectively obtained visual fields and the objectively obtained visual fields were concordant in patients with hemianopsia. In addition, we examined whether the discordance of the subjective and objective visual fields was related to the location of the lesion giving rise to the hemianopsia.

0002-9394/07/$32.00
doi:10.1016/j.ajo.2006.10.042

TABLE 1. Demographics and Summary of the Findings of mfVEP and Diagnosis of the Patients

Patient No	Age	Gender	Visual Field Loss	Diagnosis	mfVEPs (Concordance or Not)
1	51	F	Btemp. h.	Pituitary adenoma	Yes
2	49	M	Btemp. h.	Pituitary adenoma	Yes
3	38	F	Rt. homo. h.	Skull base meningioma	Yes
4	60	F	Lt. homo. h.	Brain meta (rt. parieto-occipital)	Yes
5	49	M	Lt. homo. h.	Craniopharyngioma	Yes
6	46	M	Rt. homo. h.	Meningioma (lt. occipital)	No
7	28	M	Lt. homo. h.	AVM postoperatively (rt. occipital)	No
8	68	M	Lt. homo. h.	Glioma (rt. occipital)	No
9	35	M	Rt. homo. h.	Cavernous hemangioma (lt. occipital)	No
10	30	F	Lt. homo. h.	Subarachnoid hemorrhage postoperatively (rt. occipital)	No

mfVEP = multifocal visual evoked potentials; M = male; F = female; btemp. h = bitemporal hemianopsia; rt. homo. h = right homonymous hemianopsia; lt. = left; AVM = arteriovenous malformation.

Concordance or not: "yes" means that no mfVEP response was observed at the area of visual field deficit. "no" means that mfVEP response was observed at the area of visual field deficit.

METHODS

• SUBJECTS: All of the research procedures conformed to the guidelines of the Declaration of Helsinki, and an informed consent was obtained from all subjects after an explanation of the purpose and the procedures to be used in the experiments. The mfVEPs were recorded from 10 consecutive patients who had hemianopsia, either a complete hemianopsia or quadrantanopsia, which was documented by conventional perimetry. The examinations were performed between January 1999 and February 2004 at the Keio University Hospital. The patients consisted of six men and four women whose ages ranged from 28 to 68 years with a mean of 45.4 ± 12.8 years (± standard deviation [SD]; Table 1). Three of the patients had a right and five patients had a left homonymous hemianopsia. The two remaining patients had bitemporal hemianopsia. All patients had evidence of damage to the visual pathway by computed tomography (CT) or magnetic resonance imaging (MRI), or both, which could accounted for the visual field deficits. The causes of the visual impairment were brain tumors, cerebral infarctions, or postneurosurgery for either arteriovenous malformation or subarachnoid hemorrhage. The temporal crescent syndrome was ruled out in patients with posterior lesions by CT or MRI findings.

All patients had a routine ophthalmologic examination including slit-lamp biomicroscopy, ophthalmoscopy, and attenuation tonometry. All patients had a corrected visual acuity of 20/20 or better and a refractive error of less than −5.25 diopters in both eyes. There was no history of ophthalmologic abnormalities such as glaucoma or diabetic retinopathy that could affect the visual function especially the visual fields. The perimetric examinations and mfVEPs recordings were carried out during the same period. Normative data were collected from 10 healthy eyes except for refractive error, although the age did not match the patients (age range, 27 to 65; 35.6 ± 11.6).

Because the SDs of the amplitudes of the multifocal electroretinograms (mfERGs) were relatively large (see Supplemental Table 1 available at AJO.com) in normal subjects, the ratio of the amplitudes or implicit times from horizontally adjacent quadrants was calculated. For example, the ratio of the amplitude of the summed response from superior nasal quadrant was compared with that from the superior temporal quadrant, the SN/ST ratio. The ratios of the amplitudes of the mfVEPs in the inferior nasal to inferior temporal ratio (IN/IT) were calculated in the same way. The SN/ST and IN/IT ratios of the implicit times were also calculated for R1 and R2. It was reported,[16,24,25] and confirmed here, that the general shape of the summed responses of the temporal and nasal visual fields are very similar, whereas those of the superior and inferior visual fields differed in phase and amplitude in normal subjects.

• STIMULUS FOR MFVEPS: The stimulus was similar to that used in Klistner protocol, with a dartboard pattern consisting of 61 sectors that was created on a computer monitor (17 inch, high-resolution display, stimulation rate 75 Hz; Nanao, Ishikawa, Japan).[15] Each check was either white or black with a 92% contrast (white = 160 cd/m^2; black = 7 cd/m^2), and the luminance alternated pseudorandomly at 75 frames per second. The m binary sequence was repeated two times.[16]

The individual kernels of the responses were determined by cross-correlating the digitized output signal with the binary input sequences using a fast Walsh transform. As shown in the Supplemental Figures 1 and 2 (available at AJO.com), the size of each segment was cortically scaled with eccentricity to stimulate approximately equal areas of cortical (striate) surface.[15,18,26–29] The overall stimulus subtended approximately 25 degrees at the eye.

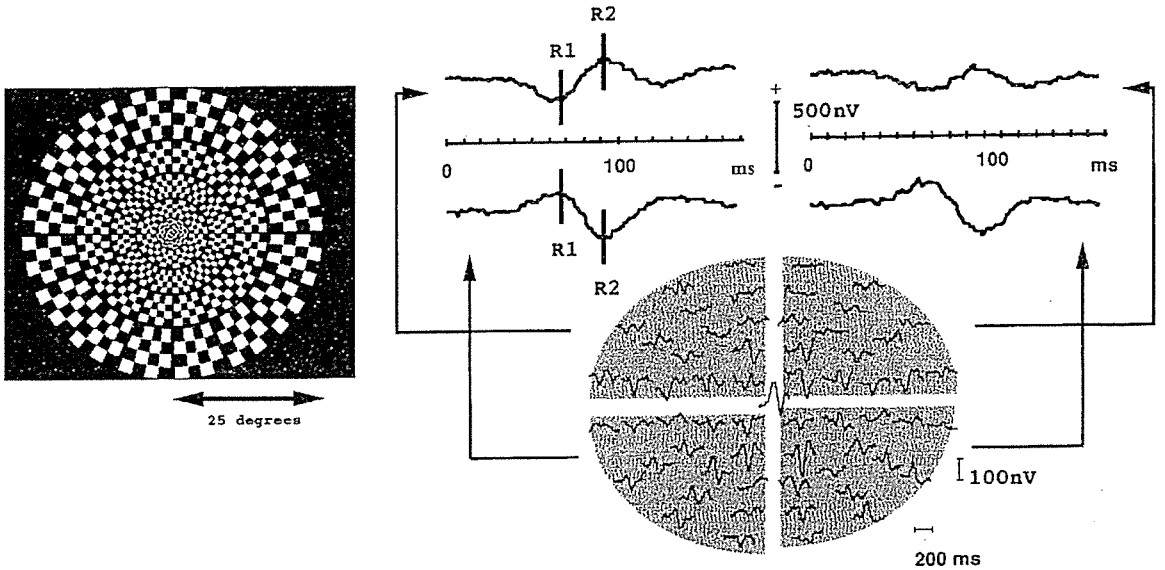

FIGURE 1. Stimulus for multifocal visual-evoked potentials. (Left) Stimulus was a dartboard pattern consisting of 61 sectors. (Right) Individual second-order kernels of the multifocal visual evoked potentials (mfVEPs) are plotted retinotopically in the lower half. The sums of the responses in each of the four quadrants are plotted in the sectors in the upper half except for the response from the very central sector.[16]

TABLE 2. The Ratio of the mfVEPs Parameters in All the Patients

			Amplitude				R1 Latency				R2 Latency			
	Conventional	Visual Field	Left Eye		Right Eye		Left Eye		Right Eye		Left Eye		Right Eye	
Case	Left Eye	Right Eye	SN/ST	IN/IT	SN/ST	IN/IT	SN/ST	IN/IT	SN/ST	IN/IT	SN/ST	IN/IT	SN/ST	IN/IT
			◪/◪	◪/◪	◪/◪	◪/◪	◪/◪	◪/◪	◪/◪	◪/◪	◪/◪	◪/◪	◪/◪	◪/◪
No.1	◐	◑	—	—	—	—	—	—	—	—	—	—	—	—
No.2	◔	◔	—	1.829	—	1.652	—	0.989	—	0.956	—	1.074	—	0.945
No.3	◑	◑	—	—	—	—	—	—	—	—	—	—	—	—
No.4	◐	◐	—	—	—	—	—	—	—	—	—	—	—	—
No.5	◐	◐	—	—	—	—	—	—	—	—	—	—	—	—
No.6	◑	◑	0.618	1.792	1.630	0.485	1.244	1.000	0.939	1.449 H	0.955	0.945	0.875 L	1.479 H
No.7	◐	◐	1.750	0.821	0.604	1.400	1.000	0.868 L	1.211	1.024	1.171 H	0.914	1.325 H	1.268 H
No.8	◐	◐	1.130	0.612	0.374	1.732	0.977	0.878 L	0.951	1.084	1.038	0.863 L	1.000	1.135 H
No.9	◔	◔	0.731	1.771	1.226	0.868	1.057	1.325 H	1.524 H	1.439 H	1.044	1.549 H	1.171 H	1.009
No.10	◴	◴	0.980	1.786	0.803	0.462	0.988	0.976	1.000	1.000	0.975	1.102	0.911 L	1.027

P1 amplitude = amplitude of the first positive component around 100 ms after stimulation; R1 latency = time interval between the stimulation and first negative component around 75 ms after stimulation; R2 latency = time interval between the stimulation and first positive component around 100 ms after stimulation; SN = superior nasal; ST = supealtemporal; IN = inferiornasal; IT = inferiortemporal.

The ratio of each mfVEPs parameters in the normal control subjects are shown in the Supplemental Table.

The mean ± 2* SD were defined as cut-off values. When the patient's ratio of any mfVEPs parameter was out of this range, it is indicated with H or L in this Table. H = the value is higher than the cut-off value; L = the value is lower than the cut-off value; — = the ratio could not be calculated because the response from the quadrant of conventional visual field defect was noise level.

To rule out cross-talk, half of the dartboard stimulus field was covered and the mfVEPs were recorded as usual. The mfVEPs usually elicited from the covered loci were completely flat.[30]

• RECORDING MFVEPS: Patients were preadapted to standard room lighting, and all recordings were performed under dim room lights. The pupils were fully dilated with 0.5% tropicamide and 0.5% phenylephrine hydrochloride. A small red fixation light was present in the center of the stimulus display, and the subjects were instructed to fixate on the red light and to try not to blink. The subjects wore their best refractive correction, and all recordings were monocular. One of the recording electrodes was placed 2.0 cm inferior to

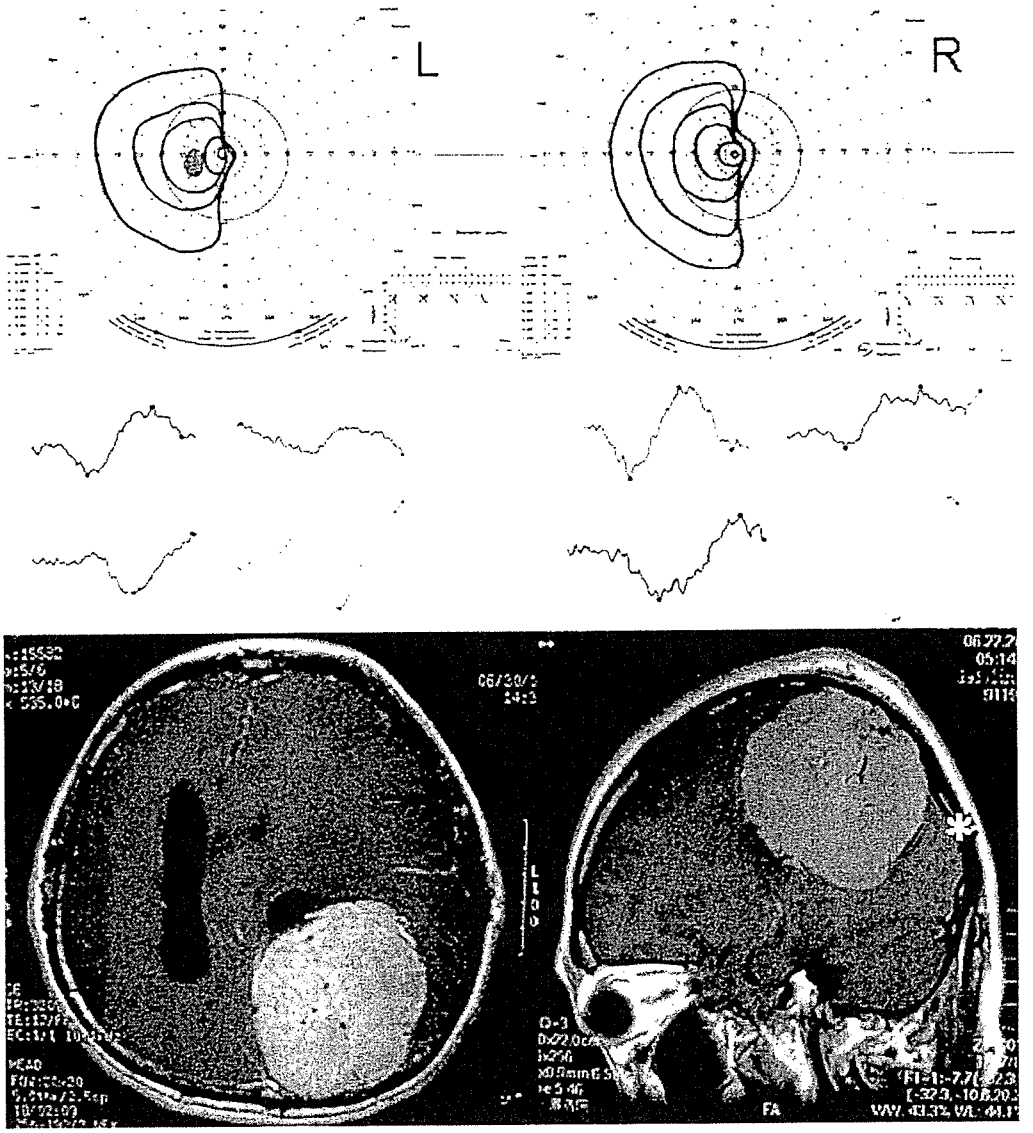

FIGURE 2. Findings in a 46-year-old man (Case 6) with right homonymous hemianopsia due to a meningioma extending from the left parietal lobe to the occipital lobe. (Top) Goldmann perimetric fields showing a left homonymous hemianopsia. (Middle) The multifocal visual evoked potentials (mfVEPs) are presented so that the average waveforms are seen in each of the quadrants where each waveform originates. The mfVEPs are not extinguished in the temporal fields of the right eye and the nasal fields of the left eye. (Bottom) An axial plane (left) and sagittal plane (right) of the magnetic resonance imaging (MRI) scan show a meningioma extending from the left parietal lobe to occipital lobe. Most of the lesion was primarily outside of primary visual cortex and in a more distal area.

(negative electrode) and the other 2.0 cm superior to (positive electrode) the inion.[15,16,32] The ground electrode was placed on the earlobe.

The mfVEPs were recorded with the VERIS II system (Tomey Co, Nagoya, Japan). Signals were amplified 50,000 times and bandpass filtered from 0.5 to 100 Hz. The sampling rate was 75 Hz, and the m-15 binary stimulation sequence was divided into 32 slightly overlapping segments. Each run was divided into eight equal segments with a total recording time of about seven minutes.

• ANALYSES: All of the mfERG data were analyzed using VERIS Science 3.01 software (Tomey Co, Nagoya, Japan).[16] The first slice of the second-order kernel was extracted and the 60 responses (omitting the central response) were divided into four quadrants and summed. Each mfVEP consisted of the R1 and R2 components that probably correspond to the N70 and P100 components of conventional VEPs (Figure 1). The implicit times and amplitudes (R2 peak − R1 peak) of R1 and R2 were calculated.

If the response of the mfVEPs was reduced in the area where an absolute scotoma was detected by conventional visual field testing, this case was considered to have a concordance between the subjective and objective visual fields. To judge whether the amplitude from the quadrant was normal, we used a criterion of <2 SDs from the same region in normal subjects (see Supplemental Table 2 available at AJO.com).

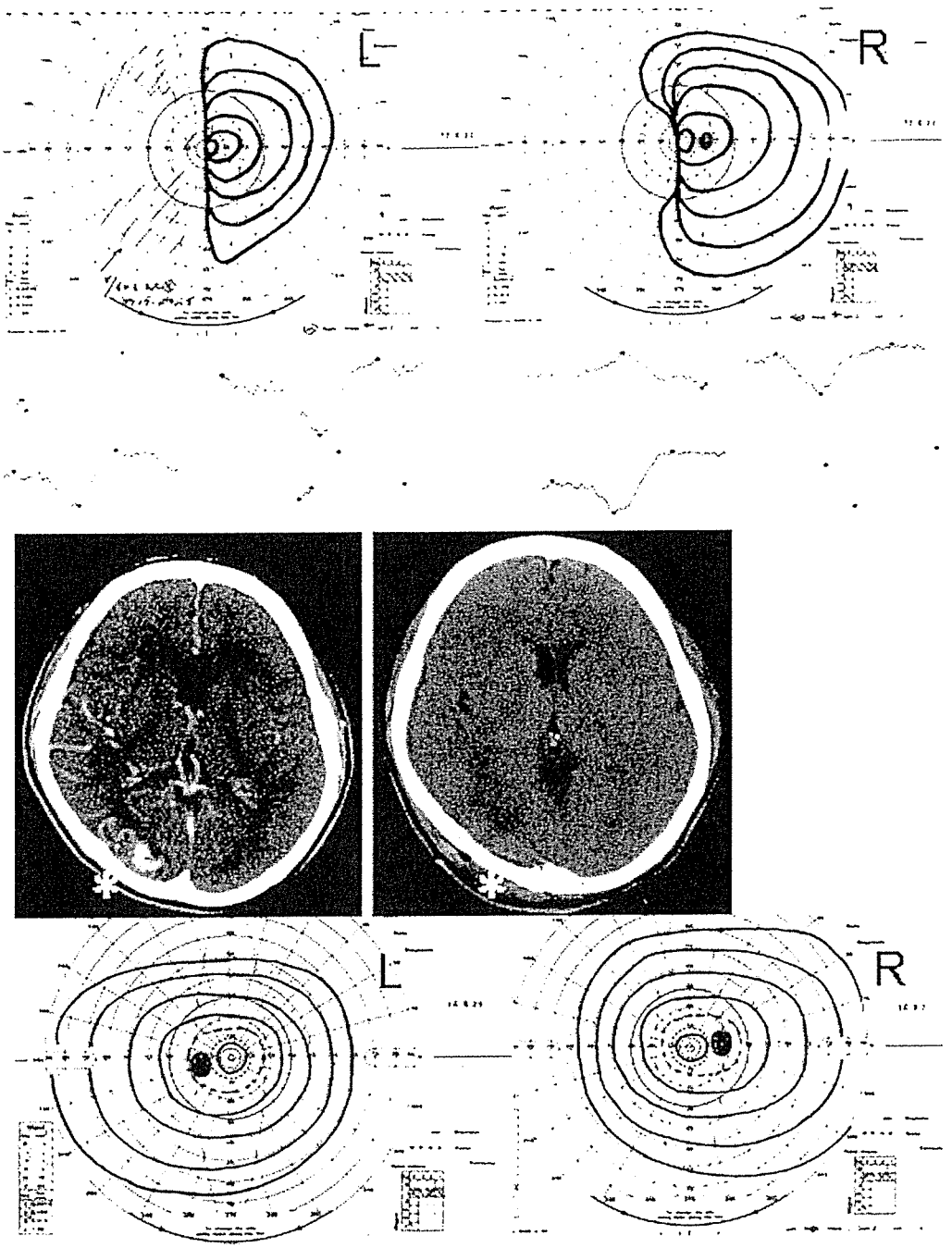

FIGURE 3. Findings in a 28-year-old man (Case 7) who underwent neurosurgery for an arteriovenous malformation in the right occipital lobe. (Top) Goldmann visual fields showing a left homonymous hemianopsia. (Second row) The multifocal visual evoked potentials (mfVEPs) are presented so that the average waveforms are seen in each of the quadrants where in the visual field each waveform originates. The mfVEPs were not extinguished in the temporal fields of the left eye and the nasal fields of the right eye. (Third row, left) Computed tomographic (CT) image showing an arteriovenous malformation in the right occipital lobe. (Third row, right) CT image showing a low-density area indicating postoperative edema in the right occipital region. (Bottom) Goldmann perimetric fields showing complete recovery of visual fields three months later.

RESULTS

THE SHAPES OF THE SUMMED MFVEPS IN THE UPPER visual field were approximately a mirror image of those in the lower field in normal subjects. This was also true for the mfVEPs elicited from the nonaffected quadrants of the patients.[16] The ratio of the mfVEPs parameters in all the patients are shown in Table 1. In some cases, the ratio could not be calculated because the mfVEP was at noise level.

A summary of our findings in the 10 cases is presented in Table 2. Five of 10 patients showed good concordance between the subjective and the objective visual fields. Thus the amplitudes of the mfVEPs were within

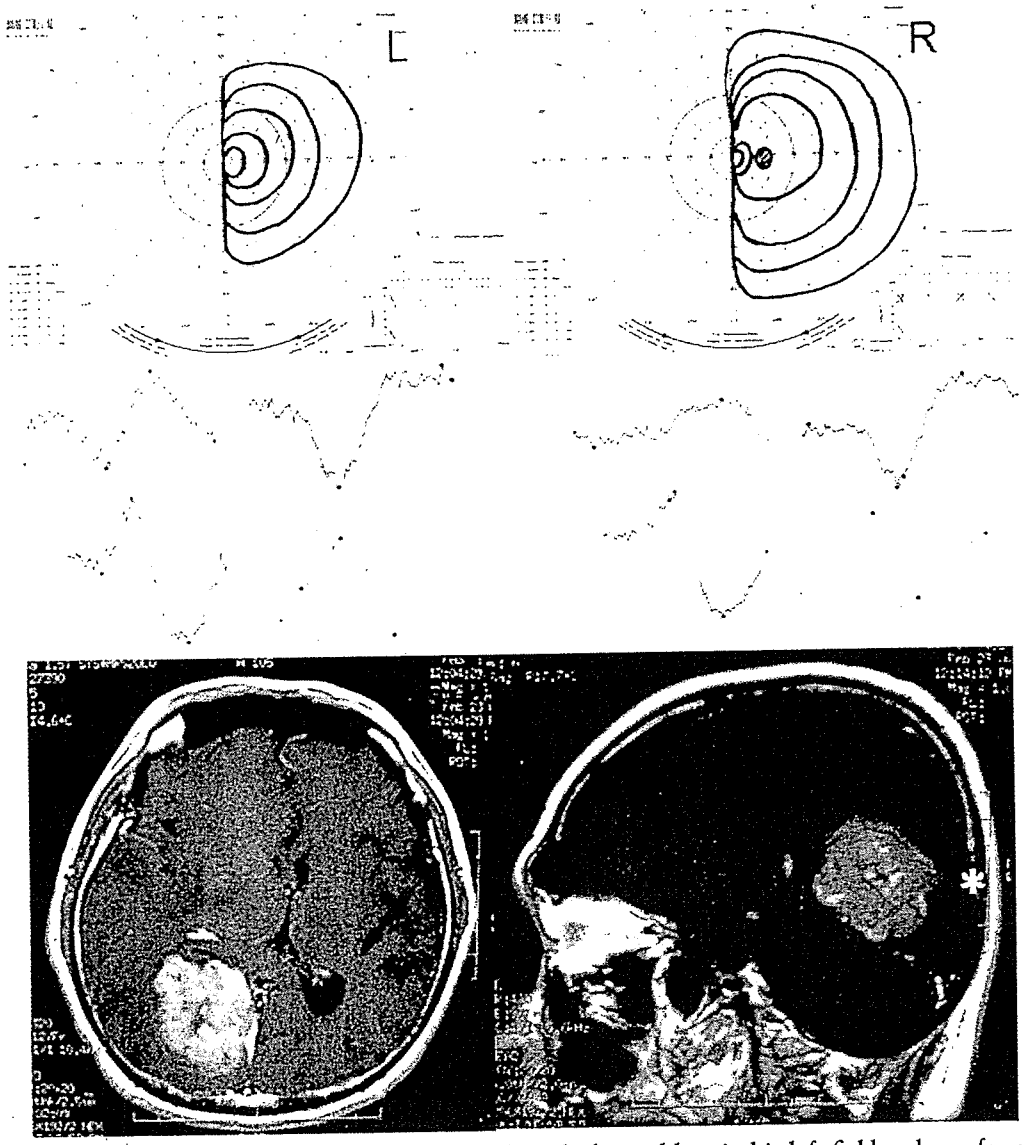

FIGURE 4. Findings in a 68-year-old-man (Case 8) who complained of visual loss in his left field and was found to have a glioma in the right occipital lobe. (Top) Goldmann perimetric fields showing a left homonymous hemianopsia. (Middle) The multifocal visual-evoked potentials (mfVEPs) are presented so that the average waveforms are seen in each of the quadrants where in the visual field each waveform originates. The mfVEPs have relatively good responses in the temporal fields of the left eye and the nasal fields of the right eye. (Bottom) An axial plane (left) and sagittal plane (right) of the magnetic resonance imaging (MRI) scan revealed a mass about 5 × 5 cm in the right occipital lobe, which was diagnosed as a glioma. Most of the lesion was primarily outside the primary visual cortex and in more distal areas.

normal limits in each quadrant in which the visual field was normal by conventional perimetry, and either the amplitude was reduced or the implicit time was delayed in the quadrants corresponding to the visual field deficits detected by perimetry. The visual field defects in these cases were due to a brain lesion outside the occipital cortex.

In contrast, the results of conventional perimetry and mfVEP topographic analysis in the other five cases were discordant. In these five patients, normal or only slightly reduced mfVEPs were recorded in the quadrants from which a subjective visual field deficit was detected. Interestingly in these cases, the site of the lesion was found in the occipital cortex in all five patients. Two of these cases (Cases 7 and 10) had a complete recovery of their visual field after the cause of the brain lesion was treated or in remission. In the five cases (Cases 1 through 5) in which the results from mfVEP were concordant with the subjective visual fields, there was no recovery of the visual fields determined by conventional perimetry.

• CASE 6: A 46-year-old man with a right homonymous hemianopsia from a meningioma. The ratios of the amplitude of the mfVEPs for SN/ST and IN/IT in the right eye were 0.618 and 1.792, respectively, whereas the normal ranges (mean ± 2 SD) were 0.311 to 1.763 and 0.155 to 1.85, respectively (Figure 2, Table 2). The ratios for SN/ST and IN/IT in the left eye were 1.630 and 0.485, respec-

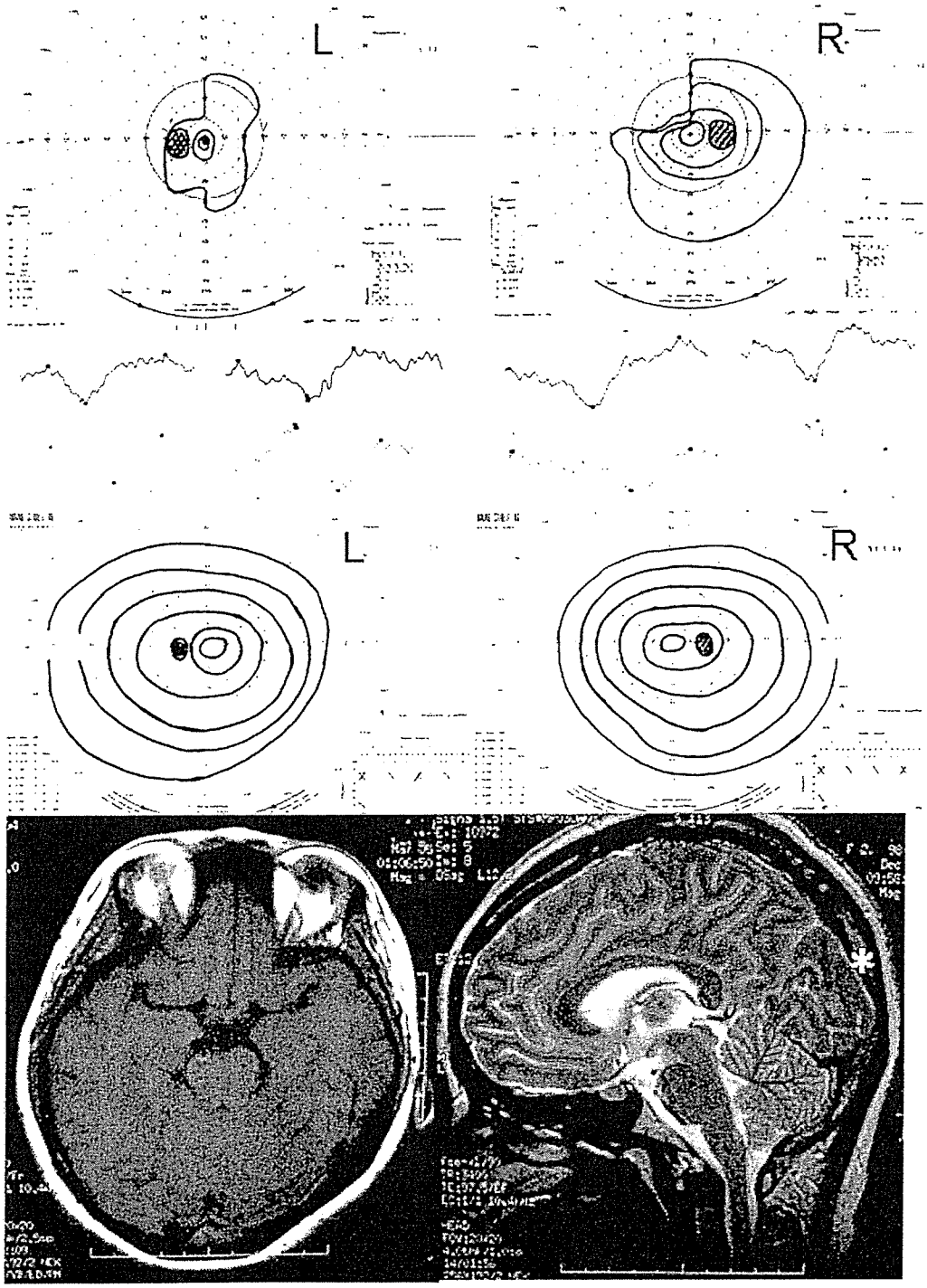

FIGURE 5. Findings in a 30-year-old-woman (Case 10) who underwent neurosurgery for subarachnoidal hemorrhage in the right occipital lobe resulting from an aneurysm of the posterior communicating artery. She complained of a visual field loss in the left field two months after surgery. (Top) Goldmann perimetric fields showing a left homonymous hemianopsia. (Second row) The multifocal visual evoked potentials (mfVEPs) are presented so that the average waveforms are seen in each of the quadrants where in the visual field each waveform originates. The mfVEPs demonstrated good responses in the nasal superior field of both eyes. (Third row) Three months later, the Goldmann fields demonstrate a complete recovery of the visual field. (Bottom right) An axial plane (left) and sagittal plane (right) of the magnetic resonance imaging (MRI) scan revealed neither particular edema nor infarction.

tively. All of these ratios were within the normal limits, suggesting that the mfVEPs were not altered in the temporal fields of the right eye and the nasal fields of the left eye. Therefore, his subjectively and objectively determined visual fields were discordant (Figure 2). His corrected visual acuity was 20/20 in both eyes, and Goldmann perimetry showed a right homonymous hemianopsia with foveal sparing. An MRI scan demonstrated a mass extending from the left parietal lobe to the occipital lobe, which was diagnosed as a meningioma.

• CASE 7: A 28-year-old man underwent surgery for an arteriovenous malformation in the right occipital lobe, and had homonymous hemianopsia postoperatively (Figure 3). The neurosurgeon referred the patient to our department for visual field examination. Examination revealed a corrected visual acuity of 20/20 in each eye, and Goldmann perimetry demonstrated a left homonymous hemianopsia. The ratios of the amplitudes of the mfVEPs for SN/ST and IN/IT in the right eye were 1.750 and 0.821, respectively (Table 2). The ratios for the left eye were 0.604 and 1.400, respectively (Table 2). All of the ratios were within the normal limits, suggesting that the mfVEPs were not altered the temporal fields of the left eye and the nasal fields of the right eye (i.e., a discordance).

Preoperative CT scan showed a nidus of about 2 × 2 cm on the right occipital lobe. CT scans seven days after the operation showed a low-density area that appeared to be postoperative edema. Goldmann perimetry showed a complete recovery of the visual fields three months after the operation.

• CASE 8: A 68-year-old man who had left homonymous hemianopsia from a glioma. The ratios of the amplitudes of the mfVEPs for SN/ST and IN/IT in the right eye were 1.130 and 0.612, respectively (Figure 4, Table 2). The same ratios for the left eye were 0.374 and 1.732, respectively. The ratios of the mfVEPs were within normal limits in the temporal field of the left eye and the nasal field of the right eye. His corrected visual acuity was 20/20 in each eye, and Goldmann perimetry showed a left homonymous hemianopsia. Therefore, his subjectively and objectively determined visual fields were concordant (Figure 4). An MRI scan revealed a mass about 5 × 5 cm in the right occipital lobe, which was diagnosed as a glioma.

• CASE 10: A 30-year-old woman who complained of a visual loss in the left field two months after neurosurgery for a subarachnoidal hemorrhage in the right occipital lobe resulting from an aneurysm in the posterior communicating artery. The neurosurgery caused a stenosis of the posterior cerebral artery. The ratios of the amplitudes of the mfVEPs for SN/ST and IN/IT in the right eye were 0.980 and 1.786, respectively. These findings indicate that the mfVEPs were not altered in the right eye even in the superior nasal visual field (Figure 5, Table 2). The ratios of the amplitude in the left eye were 0.803 and 0.462, respectively. The Goldmann visual field of the left eye showed reduced sensitivities in all the quadrants. The mfVEP amplitude for each quadrant was normal. She had a left homonymous hemianopsia with reduced sensitivities in the left eye postoperatively that showed discordance in both eyes (Figure 5). Her corrected visual acuity was 20/20 in each eye. Goldmann perimeter showed a left homonymous hemianopsia and concentric visual field deficit in the left eye. An MRI scan revealed neither edema nor infarction. Five months later, Goldmann perimetry demonstrated a complete recovery of the visual fields.

DISCUSSION

WE HAVE EVALUATED THE MFVEPS RECORDED WITH BIpolar occipital electrodes that straddled the inion and were elicited by a pseudorandom binary m sequence.[16] Our earlier results with the same stimulus and recording protocols showed that the summed mfVEPs in the four quadrants were highly concordant with the results of conventional subjective perimetry. Therefore, we concluded that this technique can be used to assess the visual field defects objectively in patients with diseases in the visual pathway.

However, as the number of such patients increased, we encountered some cases in which the mfVEPs were less impaired or even within normal limits in spite of visual field defects detected by conventional perimetry. We found that these discordant cases always had a lesion in the occipital area. However, the patients with homonymous hemianopsia from an occipital lesion did not always show such disagreement between subjective and objective visual fields.

The origin of human visual evoked potentials has been extensively investigated, and the evidence suggest that they originate from some part of the striate cortex or calcarine fissure.[14,15,26,32–34] Although the exact origin of the mfVEPs is still undetermined, they are believed to be mainly derived from area V1 of the striate cortex.[35–38] Therefore, mfVEPs and subjective visual field should be impaired from pathologic lesions in this area. If any part of the visual pathway before V1 is involved, the mfVEP recorded should be abnormal in the quadrants corresponding to the visual field defects, as seen in cases 1 and 2 in which chiasmal lesion led to bitemporal hemianopsia. In case 3, with a meningioma at the base of the skull, the mfVEPs were reduced in agreement with the homonymous left hemianopsia detected by Goldmann perimetry. This concordance can be reasonably explained by the postchiasmal damage of the visual pathway before V1.

However, localized damage of higher visual centers (e.g., V2/V3) can cause visual field defects when determined by perimetry but not by mfVEPs. We suggest that the discordance between the subjectively and objectively determined visual fields observed in the five cases was because the lesion was in the post-striate cortex. In the two cases (Cases 7 and 10) that had significant improvements of the visual field after a resolution of the brain lesion, we suggest that the postsurgical edema (Case 7) was the cause of the early visual field defect.

Klistner and associates recorded normal mfVEPs in patients with quadrantanopia that were consistent with an extrastriate lesion that was very congruous, complete, and respected the horizontal meridian. They stated that